DOI 10.1007/s10946-017-9622-z
Journal of Russian Laser Research, Volume 38, Number 1, January, 2017

26 mJ TOTAL OUTPUT FROM A GAIN-SWITCHED SINGLE-MODE Er^{3+}-DOPED ZBLAN FIBER LASER OPERATING AT 2.8 μm

Yanlong Shen,* Ke Huang, Kunpeng Luan, Yang Zhu, and Li Yu

State Key Laboratory of Laser Interaction with Matter
Northwest Institute of Nuclear Technology
P.O. Box 69-18, Xi'an 710024, P. R. China

*Corresponding author e-mail: yanlong_xian@126.com

Abstract

We demonstrate a laser-diode-pumped gain-switched Er^{3+}-doped ZrF_4-BaF_2-LaF_3-AlF_3-NaF (ZBLAN) fiber laser operating in a single transverse mode at 2.8 μm. The laser pulses produced offer high-pulse energies, with repetition rates ranging from 50 Hz to 10 kHz and a slope efficiency of approximately 14.3% with respect to the launched pump power. The average power at the 50 Hz repetition rate is 1.33 W, giving a maximum total output pulse energy of 26.6 mJ per pump pulse. The fiber laser operates in a single mode, with beam quality factor M^2 less than 1.2.

Keywords: high-energy gain-switched diode-pumped Er:ZBLAN fiber laser.

1. Introduction

Recently, rare-earth-ion-doped fluoride fiber lasers emitting in the mid-infrared (mid-IR) waveband have received considerable interest from researchers because of their potential for applications in fields such as medicine [1], IR laser pumping [2], and spectroscopy [3].

Highly Er^{3+}-doped ZrF_4-BaF_2-LaF_3-AlF_3-NaF (ZBLAN) fiber lasers operating on the $^4I_{11/2} \rightarrow {}^4I_{13/2}$ transition at 2.8 μm have become the most promising candidates for use in these applications, because these fiber lasers offer an excellent combination of high efficiency, outstanding beam quality, and a broad-emission spectral range [4]. The coincidence of the Er^{3+} ion's convenient 975 nm pump band with the wavelengths of high-power laser diodes available as pumping sources means that significant progress has been made in the development of Er^{3+}-doped ZBLAN fiber lasers in the continuous wave (CW) regime over the past decade [5–8]. Zhu et al. obtained 9 W output in the CW regime with a slope efficiency of 21% at room temperature [5]. Most importantly, a fiber Bragg grating was first written successfully in ZBLAN fibers in 2007 [9], and thus can be used to construct highly efficient and tunable all-fiber mid-IR fiber lasers. Accordingly, Fortin et al. demonstrated a 20 W all-fiber Er^{3+}-doped ZBLAN mid-IR fiber laser in 2011 [10], and they recently also claimed a maximum recorded output power of 30 W [11].

For many applications, however, such as medical surgery or damage measurement, pulsed lasers are preferred to CW mode lasers because of advantages that include high precision, high sensitivity, and high response speeds [12]. Two principal methods, i.e., Q-switching and mode locking, are commonly used to produce pulsed laser outputs [13,14]. A number of actively and passively Q-switched Er^{3+}-doped fluoride fiber lasers emitting at 2.8 μm have been demonstrated during the past few years [15–19]. The

Manuscript submitted by the authors in English first on November 1, 2016 and in final form on December 15, 2016.

first actively Q-switched fluoride fiber laser operating in the 3 μm region with an acousto-optic modulator was reported in early 1994 [15]. An actively Q-switched Er^{3+}-doped ZBLAN fiber laser emitting at 2.8 μm with a pulse energy of 100 μJ, an average power of 12 W, and a peak power of 0.9 kW, was obtained in 2011 [16].

In terms of passively Q-switched Er^{3+}-doped ZBLAN fiber lasers, many such lasers were demonstrated based on the use of various saturable absorbers, including InAs epilayers [17], Fe^{2+}:ZnSe crystals [18], graphene [19], and semiconductor saturable-absorber mirror (SESAM) technology [20]. Wei et al. demonstrated a passively Q-switched Er^{3+}-doped ZBLAN fiber laser with a pulse width of 800 ns and a pulse energy of 460 nJ at a repetition rate of 105 kHz using a Fe^{2+}:ZnSe crystal [18]. Replacing this Fe^{2+}:ZnSe crystal by graphene, they also produced passively Q-switched pulses [19]. Shen et al. reported a watt-level SESAM-based purely passively Q-switched Er^{3+}-doped ZBLAN fiber laser with a maximum pulse energy of 6.9 μJ and a peak power in excess of 21 W using a short 0.9 m fiber, which represented the maximum average power and peak power achieved in the 3 μm waveband using passively Q-switched fiber lasers to date [20].

Following the emergence of new materials for use as saturable absorbers, topological insulators and black phosphorus have very recently been shown to be capable of generating mid-IR laser pulses [21, 22]. In terms of mode-locked operation, several researchers have demonstrated passively mode-locked mid-IR fiber lasers with pulse widths on the ps scale and peak powers on the kW scale when using a SESAM [23] and nonlinear polarization rotation techniques [24].

Nevertheless, Q-switching and mode locking have certain disadvantages when used in fluoride fiber lasers to obtain high output pulse energy [25], including cavity complexity and risk of damage to the active fiber. To date, 2.8 μm pulsed ZBLAN fiber lasers have produced pulses of short duration at high repetition rates. In many cases, high repetition rates are both unsuitable and unnecessary, and longer pulses with higher pulse energies would be desirable for certain medical applications [26]. Because it is pumped directly by a pulsed laser diode, the gain-switched fiber laser offers a rather simple way to produce high-energy pulses with suitably controllable repetition rates. In 2001, Dickinson et al. reported a gain-switched Er^{3+}/Pr^{3+}-codoped ZBLAN fiber laser operating at 2.7 μm that was pumped by a pulsed Ti:sapphire laser with a pulse energy of 1.9 mJ and pulse width of 18 μs [25]. Gorjan et al. demonstrated an average power of 2 W at a repetition rate of 100 kHz in gain-switched operation and obtained a maximum pulse energy of 0.4 mJ [27].

In this work, we report a total output of 26 mJ from a gain-switched Er^{3+}-doped double-clad ZBLAN fiber laser on the $^4I_{11/2} \rightarrow ^4I_{13/2}$ transition at 2.8 μm; the fiber laser was pumped by a pulsed laser diode that was centered at 975 nm with relatively low repetition rates (RRs) ranging from 50 Hz to 10 kHz. A maximum total output energy per pump pulse of 26.6 mJ was obtained. The laser beam quality factor (M^2) was measured to be less than 1.2.

2. Experimental Setup

The experimental setup used for the gain-switched Er^{3+}-doped ZBLAN fiber laser is depicted schematically in Fig. 1. A fiber-coupled laser diode with a central wavelength of approximately 975 nm and a maximum CW output power of 50 W was used as the pulsed pump source with a custom designed low RR range of 50 Hz – 10 kHz. The pigtail fiber of this laser diode had a core diameter of 105 μm and a numerical aperture (NA) of 0.22. The active fiber (fabricated by FiberLabs, Inc.) was a heavily Er^{3+}-doped ZBLAN double-clad fiber that was approximately 4.6 m long. The fiber core specifications were as follows: diameter, 17 μm; NA, 0.12; and ErF_3 concentration 6 mol.%. The core has a V-value of 2.29 at 2.8 μm, which allows the 2.8 μm signal to operate in a single transverse mode. The inner cladding of the fiber was chosen to be octagonal, and the side dimension and NA of the cladding were 330 μm and 0.55, respectively. The outer circular cladding had a diameter of 370 μm. The fiber ends were held by fiber chuck holders with U-shaped groove heat sinks. The absorption coefficient of this singly Er^{3+}-doped ZBLAN fiber was determined to be 2.2 dB/m. The pulsed 975 nm LD pump beam was coupled into the inner cladding of the active fiber using a coupling system that was composed of a collimator and an aspherical lens. The sides of the lenses were antireflection-coated at the pump wavelength. Using this pump configuration, we measured the coupling system efficiency to be approximately 80%.

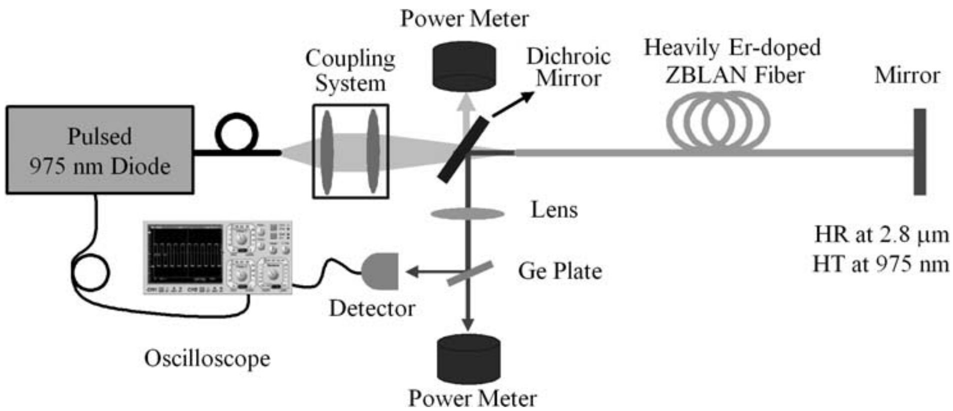

Fig. 1. Schematic layout of experimental setup for the gain-switched Er^{3+}-doped ZBLAN fiber laser.

A dielectric-coated mirror with reflection of ∼95% at 2.8 μm and high 975 nm transmittance was directly butted against the rear end of the fiber. The other end of the fiber, i.e., the pumping end, was carefully cleaved using a fiber cleaver (3SAE Inc., USA) at 0° (the angle between the optical axis of the fiber and the normal vector of the cleaved surface) to serve as the laser output port with an output efficiency of nearly 96% (Fresnel reflection ∼4%). A dichroic mirror (high reflection of ∼ 99% at 2.8 μm, high transmittance of > 95% at 975 nm) was placed in front of the pumping end with an angle of incidence of 45° to couple out the laser beam energy. The launched pump power was monitored using a fraction (∼1%) of the pump beam, which was reflected by the dichroic mirror and measured using a power meter (OPHIR, 3A-P-V1). A CaF_2 lens with a focal length of 50 mm was used to collimate the laser beam. An uncoated 2 mm thick Ge plate (transmittance of ∼ 45% at > 2 μm; transmittance of ∼ 0 at < 1.8 μm) was used to purify and split the laser beam. The output power was measured using another power meter (Gentec, UP19k-50L-H5), and the laser pulse was detected using a HgCdTe detector (Vigo PVM-2TE-10.6-2, with rise time of ∼ 3 ns); the waveforms of both the pulsed pump signal and the laser signal were captured synchronously using a 1 GHz oscilloscope (LeCroy 6100A). The output spectrum and the beam shape were recorded using an optical spectrum analyzer (Andor Shamrock 750) with resolution as high as 0.2 nm and a pyroelectric array camera (Spiricon), respectively.

3. Results and Discussion

Operation of the gain-switched 2.8 μm fiber laser was easily achieved using moderate pump energy. The temporal characteristics of the gain-switched fiber-laser pulses for different output powers at an RR of 10 kHz are as shown in Fig. 2. At output powers of less than 35.5 mW, there was only one laser pulse per pump period. The pump power was increased until the output power exceeded 35.5 mW, and then multiple pulses occurred. Higher pump powers led to shorter build-up times (i.e., the time between the pump starting and the first pulse), and more multi-pulses then appeared.

The output pulse in the gain-switching mode is actually the first pulse of the laser relaxation oscillations, and if the pump is not switched off or the pump energy exceeds a specific value (the energy still stored in the upper laser level after the first laser pulse), multiple pulses from further oscillations, i.e., pulse spikes (see Fig. 2), will follow with decreasing peak powers until the laser reaches the CW regime [27].

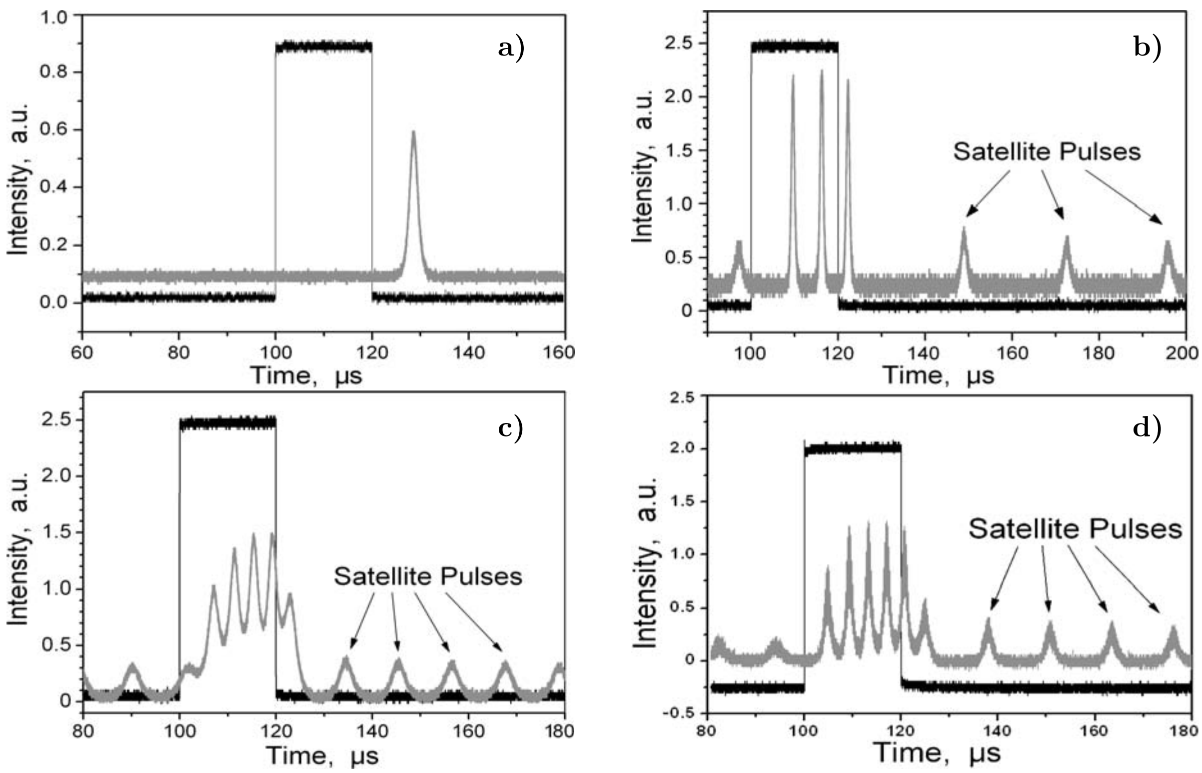

Fig. 2. Measured temporal characteristics of laser pulses with various output powers of 7.8 mW (a), 37.7 mW (b), 508.3 mW (c), and 1.3 W (d) at 10 kHz (pump: black line; laser: grey line).

From Fig. 2, it could also be seen that, following the main gain-switched envelopes at a time interval of tens of microseconds, there were still some satellite pulses. These pulses indicated that energy was still stored in the $^4I_{13/2}$ level and the upper laser $^4I_{11/2}$ level was repopulated through energy-transfer up-conversion between the particles in the lower laser $^4I_{13/2}$ level before being depleted again, and thus releasing the satellite pulses [28]. Higher pump energies caused more satellite pulses to appear, and their amplitudes were closer to that of the main envelope.

The typical pulse profiles obtained at various RRs are shown in Fig. 3 at an output power of 1.3 W. To produce the same output power, the pump power at each RR was approximately 8.1 W. At this pumping level, the laser pulse width was almost the same as the pump pulse width at each RR.

The output laser powers are shown at different pump RRs in Fig. 4. The average power increased almost linearly with increasing launched pump power, and the slope efficiency was determined to be

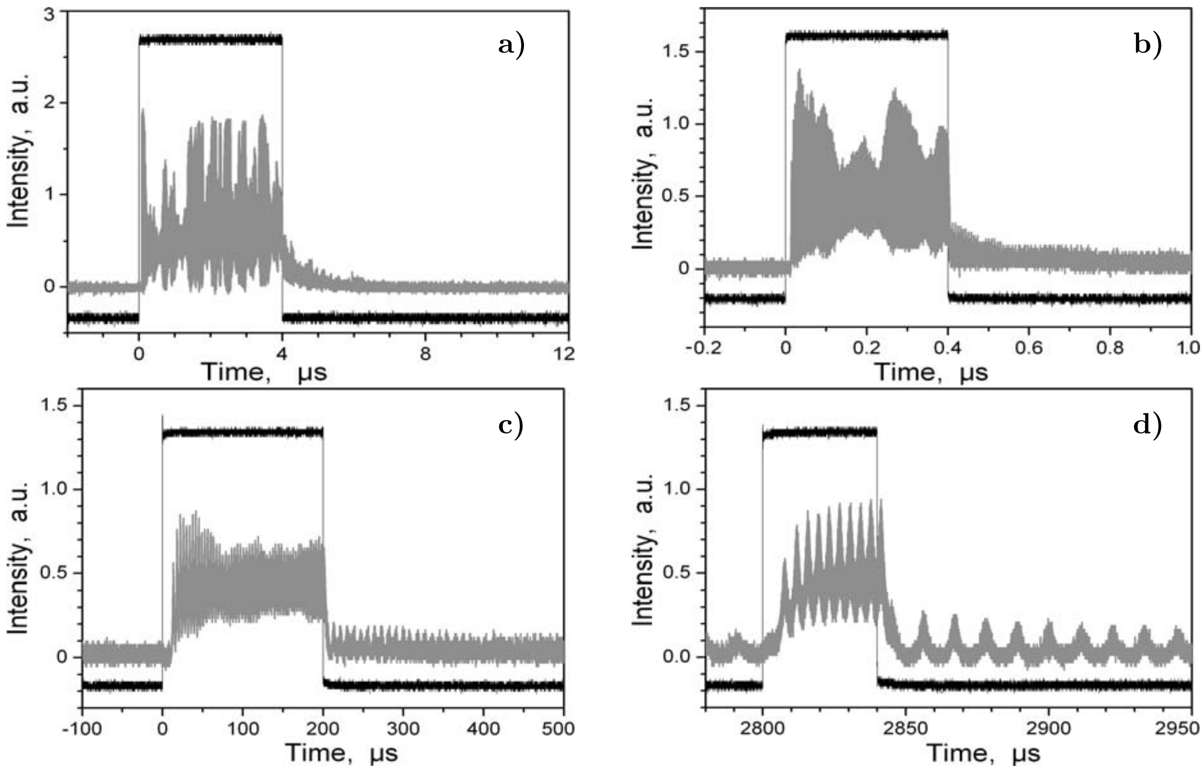

Fig. 3. Measured temporal characteristics of laser pulses with repetition rates of 50 Hz (a), 500 Hz (b), 1 kHz (c), and 5 kHz (d) at an output power of 1.3 W (pump: black line; laser: grey line).

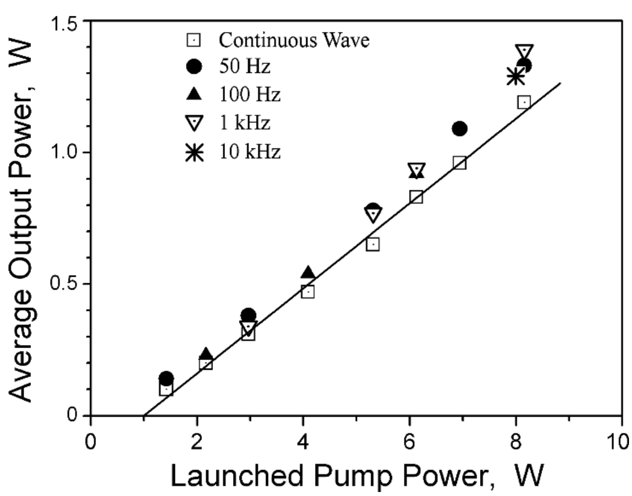

Fig. 4. Measured average output laser power vs. average launched pump power in various regimes. The solid curve represents fitting of the output power in the CW regime, showing a slope efficiency of 14.3%.

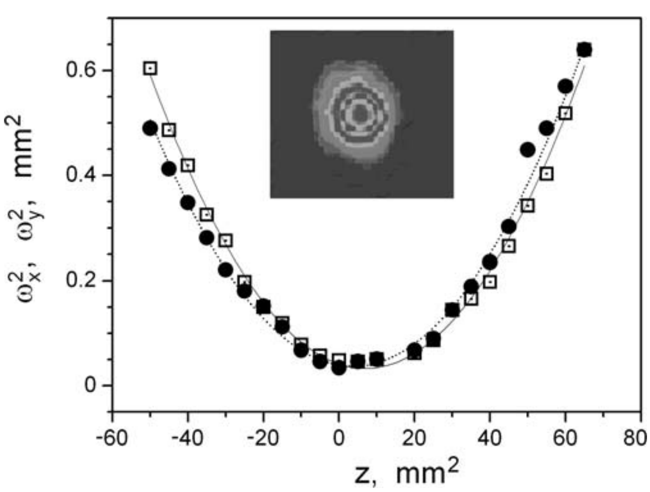

Fig. 5. Laser beam radius as a function of the distance from the waist location at $z = 0$ for x coordinate (□, $M_x^2 < 1.1$ – solid curve) and for y coordinate (•, $M_y^2 < 1.2$ – dotted curve). Inset: far-field image of the laser beam at maximum output power.

approximately 14.3% in the CW regime; this was lower than the Stokes efficiency limit of 34.8%, mainly because of the relatively low reflection at the laser wavelength, the high transmittance of the rear mirror at the pump wavelength, and the low absorption efficiency of the pump. The maximum output power was 1.33 W at a repetition rate of 50 Hz, providing a single pulse energy of 26.6 mJ, which is to our knowledge the highest total output pulse energy reported in mid-IR fiber lasers.

In the case where the light is transported by a single-mode fiber (SMF), the theoretical beam quality is typically close to the diffraction limit, i.e., $M^2 \approx 1$. To confirm that the output beam was in a single mode and to measure the beam quality factor M^2, we performed ISO-standard caustic measurements [29]; the results of these measurements are shown in Fig. 5. The far-field beam spot has a symmetrical Gaussian distribution, which indicates that the laser beam is in the TEM_{00} mode. Using a nonlinear fit, we calculated the beam quality M^2 to be less than 1.2.

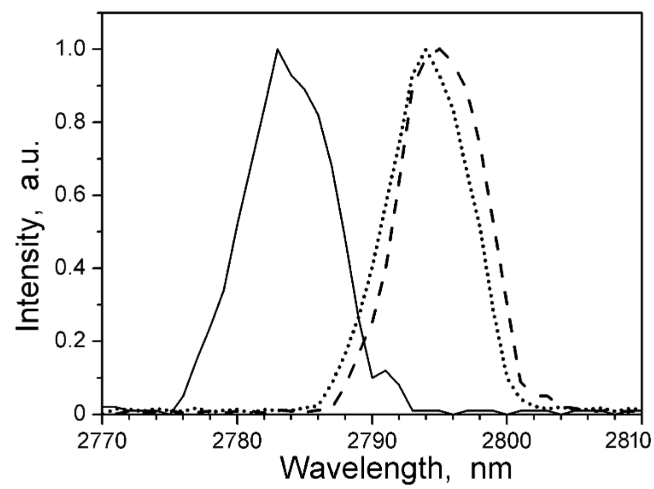

Fig. 6. Output spectra at various output powers equal to 0.2 W (solid curve), 0.7 W (dotted curve), and 1.1 W (dashed curve) at $f = 10$ kHz.

The laser output spectra for various output powers at an RR of 10 kHz are shown in Fig. 6. The central wavelength is 2783.1 nm, with a line width of approximately 5.8 nm at a low output power of 0.2 W, and the wavelength shifted to 2794.3 nm at a high output power of 1.3 W with increasing pump power. This phenomenon is very common in fiber lasers without wavelength selection elements inserted in the cavity, and is also named the red shift. Consequently, by replacing the rear mirror with a blazed grating to provide feedback, the output wavelength can be locked and the line width becomes much narrower [30].

4. Conclusions

In conclusion, we report 26.6 mJ total output from a gain-switched single-mode Er^{3+}-doped ZBLAN fiber laser output when pumped using an active pulsed diode system. We believe that the fiber laser presented here delivers the highest reported total output pulse energy for mid-IR fiber lasers. The maximum pulse energy obtained is 26.6 mJ at a rather low repetition rate of 50 Hz. The slope efficiency of the pulsed regime is approximately 14.3% with respect to the launched pump energy, which is also slightly higher than that of the CW regime. The fiber laser system proposed represents a high pulse energy laser source for potential use in medical applications.

Acknowledgments

This work is financially supported by the fund of the State Key Laboratory of Laser Interaction with Matter under Grant No. SKLLIM1503. The authors are grateful to Yongsheng Zhang from the State Key Laboratory of Laser Interaction with Matter (Northwest Institute of Nuclear Technology) for fruitful discussions.

References

1. M. Skorczakowski, J. Swiderski, W. Pichola, et al., *Laser Phys. Lett.*, **7**, 498 (2010).
2. X. S. Zhu and N. Peyghambarian, *Adv. Optoelectron.*, **2010**, 501956 (2010).
3. S. D. Jackson, *Nature Photon.*, **6**, 423 (2012).
4. X. Zhu and R. Jain, *Appl. Opt.*, **45**, 7118 (2006).
5. X. Zhu and R. Jain, *Opt. Lett.*, **32**, 26 (2007).
6. S. Tokita, M. Hirokane, M. Murakami, et al., *Opt. Lett.*, **35**, 3943 (2010).
7. X. Zhu and R. Jain, *Opt. Lett.*, **32**, 2381 (2007).
8. S. Tokita, M. Murakami, and S. Shimizu, *Opt. Lett.*, **34**, 3062 (2009).
9. M. Bernier, D. Faucher, R. Vallée, et al., *Opt. Lett.*, **32**, 454 (2007).
10. D. Faucher, M. Bernier, and G. Androz, *Opt. Lett.*, **36**, 1104 (2011).
11. V. Fortin, M. Bernier, S. T. Bah, and R. Vallée, *Opt. Lett*, **40**, 2882 (2015).
12. J. F. Li, H. Y. Luo, Y. L. He, et al., *Laser Phys. Lett.*, **11**, 065102 (2014).
13. C. Wei, X. Zhu, R. A. Norwood, and N. Peyghambarian, *IEEE Photon. Technol. Lett.*, **24**, 1741 (2012).
14. T. Hu, S. D. Jackson, and D. D. Hudson, *Opt. Lett.*, **40**, 4226 (2015).
15. C. Frerichs and T. Tauermann, *Electron. Lett.*, **30**, 706 (1994).
16. S. Tokita, M. Murakami, S. Shimizu, et al., *Opt. Lett.*, **36**, 2812 (2011).
17. C. Frerichs and U. B. Unrau, *Opt. Fiber Technol.*, **2**, 358 (1996).
18. G. Zhu, X. Zhu, K. Balakrishnan, et al., *Opt. Mater. Express*, **3**, 1365 (2013).
19. C. Wei, X. Zhu, F. Wang, et al., *Opt. Lett.*, **38**, 3233 (2013).
20. Y. Shen, Y. Wang, K. Luan, et al., *Sci. Rep.*, **6**, 26659 (2016).
21. J. Li, H. Luo, L. Wang, et al., *Opt. Lett.*, **40**, 3659 (2015).
22. Z. Qin, G. Xie, H. Zhang, et al., *Opt. Express*, **23**, 24713 (2015).
23. P. Tang, Z. Qin, J. Liu, et al., *Opt. Lett.*, **39**, 3294 (2014).
24. S. Duval, M. Bernier, V. Fortin, et al., *Optica*, **2**, 623 (2015).
25. B. Dickinson, P. Golding, M. Pollnau, et al., *Opt. Commun.*, **191**, 315 (2001).
26. W. Xuedong, Z. Xiaobing, Z. Xiaopeng, and S. Ruifeng, *Rare Metal Mater. Eng.*, **42(S2)**, 205 (2013).
27. M. Gorjan, R. Petkovšek, M. Marinček, and M. Čopič, *Opt. Lett.*, **36**, 1923 (2011).
28. H. Tsao, C. Chang, S. Lin, et al., *Opt. Laser Technol.*, **56**, 354 (2014).
29. D. Flamm, C. Schulze, R. Brüning, et al., *Appl. Opt.*, **51**, 987 (2012).
30. F. Wang, D. Shen, D. Fan, and Q Lu, *Opt. Express*, **18**, 8937 (2010).